Adsorption Properties of Novel Chelating Resins Containing 2-Amino-5-Methylthio-1,3,4-Thiadizole and Hydrophilic Spacer Arms for Hg^{2+} and Ag^+

Chunrong Wang, Chunnuan Ji, Yanfeng Meng, Li Liu, Rongjun Qu, Chunhua Wang

School of Chemistry and Materials Science, Ludong University, Yantai 264025, China

ABSTRACT: The adsorption properties, including the adsorption kinetics, adsorption isotherms, and adsorption selectivity, of newly formed chelating resins that contained a heterocyclic functional group and a hydrophilic spacer arm of poly(ethylene glycol) [polystyrene–diethylene glycol–2-amino-5-methylthio-1,3,4-thiadizole (PS–DEG–AMTZ) and polystyrene–triethylene glycol–2-amino-5-methylthio-1,3,4-thiadizole (PS–TEG–AMTZ)] were studied in detail. The results show that the adsorption kinetics of PS–DEG–AMTZ and PS–TEG–AMTZ for Hg^{2+} and Ag^+ could be described by a pseudo-second-order rate equation. The introduction of a spacer arm between the polymeric matrix and functional group was beneficial for increasing the adsorption rates. The apparent activation energies of the resins for Hg^{2+} and Ag^+ were within 20.89–32.32 kJ/mol. The Langmuir model could describe the isothermal process of Hg^{2+} and Ag^+. The competitive adsorption of the resins for Hg^{2+} and Ag^+ in binary mixture systems was also investigated. The results show that Hg^{2+} and Ag^+ were adsorbed before the other metal ions, such as Cu^{2+}, Zn^{2+}, Fe^{3+}, Cd^{2+}, and Pb^{2+}, under competitive conditions. Five adsorption–desorption cycles were conducted for the reuse of the resins. The results indicate that these two resins were suitable for reuse without considerable changes in the adsorption capacity. © 2009 Wiley Periodicals, Inc. J Appl Polym Sci 116: 636–644, 2010

Key words: ion exchangers; polystyrene; resins

INTRODUCTION

There is a constant demand for chelating resins to remove heavy-metal ions selectively from medicinal, industrial, and environmental aqueous solutions. In this respect, much attention has been drawn to the synthesis of novel chelating resins and the investigation of their adsorption properties.[1–6] In general, chelating resins are prepared by the anchoring of complexing groups onto a solid support, such as a silica gel, cellulose, or macroporous copolymers.[7] Among the aforementioned solid supports, styrene–divinylbenzene copolymer has been used most widely because of its good physical and chemical properties, such as its porosity, high surface area, durability, and purity.[8] Many chelating resins have been synthesized by the direct attachment of heterocyclic functional groups, such as pyridine, imidazole, thiazole, and pyrazole, onto styrene–divinylbenzene copolymers. These resins have had excellent adsorption and selectivity properties for heavy- and noble-metal ions.[9–14] Because the nature of the polymeric matrix of styrene–divinylbenzene is hydrophobic, the hydrophobicity of the resins sometimes has made it difficult for the metal ions to diffuse into the interior of the chelating resin and coordinate with functional groups. To overcome this problem, many attempts have been made to improve the hydrophilicity of chelating resins by the introduction of hydrophilic spacer arms (e.g., ethylene oxide,[15–18] ethylene sulfur,[19] and ethylene imine[20]) between the functional group and the polymeric matrix. It was found that the introduction of a hydrophilic spacer arm could enhance the hydrophilicity and steric flexibility of the polymeric ligands and increase the adsorption capacity and adsorption kinetics of the chelating resin.

In our previous studies,[21,22] resins containing 2-amino-5-methylthio-1,3,4-thiadizole and hydrophilic spacer arms [polystyrene–diethylene glycol–2-amino-5-methylthio-1,3,4-thiadizole (PS–DEG–AMTZ) and polystyrene–triethylene glycol–2-amino-5-methylthio-1,3,4-thiadizole (PS–TEG–AMTZ); Scheme 1] were synthesized and characterized. Our preliminary experimental results show that the resins exhibited higher affinities for Hg^{2+} and Ag^+. The presence of spacer arms in the polymers between the heterocyclic
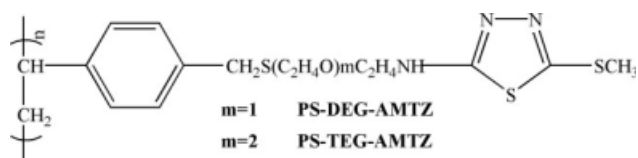
Scheme 1 Structure of PS–DEG–AMTZ and PS–TEG–AMTZ.

functional group and the polymeric matrix evidently increased the adsorption capacities for metal ions and improved the adsorption kinetics. As a successive work, this article describes the adsorption kinetics and isotherms of PS–DEG–AMTZ and PS–TEG–AMTZ for Hg^{2+} and Ag^+ at different temperatures. The apparent activation energies of PS–DEG–AMTZ and PS–TEG–AMTZ for Hg^{2+} and Ag^+ were evaluated according to an Arrhenius equation. The adsorption selectivity in binary mixture systems was also investigated with a batch experimental method.

EXPERIMENTAL

Materials

Commercial macroporous polychloromethylstyrene beads (chlorine content = 19.85%) were purchased from the Chemical Factory of Nankai University (Tianjin, China). 2-Amino-5-methylthio-1,3,4-thiadizole, 2-(2-chloroethoxy)ethanol and 2-[2-(2-chloroethoxy)ethoxy]ethanol were purchased from Aldrich Chemical Co. (USA) and were used as received. Other reagents were analytical-grade chemical products and were used without any purification.

Stock solutions of all of the metal ions were prepared by the dissolution of appropriate amounts of
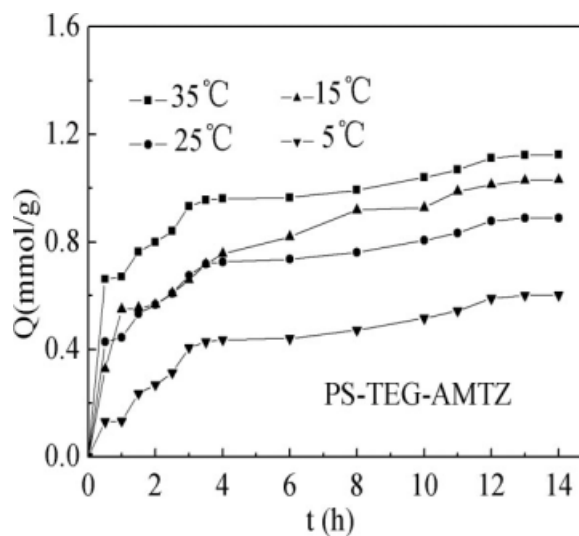

Figure 2 Adsorption kinetics of PS–TEG–AMTZ for Hg^{2+} (pH = 3, $[Hg^{2+}]$ = 0.005 mol/L).

analytical-grade nitrates in distilled water. Buffer solutions were prepared by the addition of dilute nitric acid or liquid ammonia to a 0.1M ammonium acetate solution.

Instruments

The contents of S and N elementary analyses were performed by an Elementar Analysensysteme Vario-el made in Hanau, Germany. The infrared spectra were recorded on a Nicolet Magna IR550 (series II) spectrometer (Madison, WI). The concentrations of metal ions were measured on a GBC-932 atomic absorption spectrophotometer (Victoria, Australia).
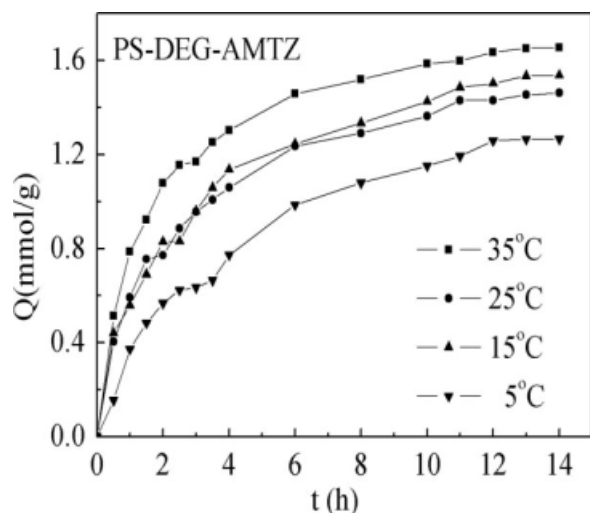

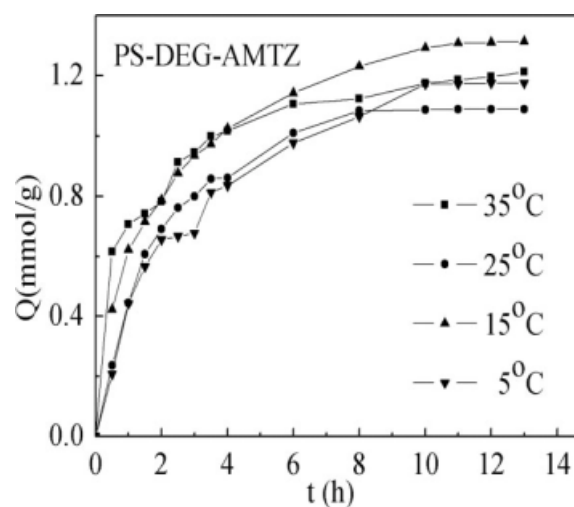**Figure 1** Adsorption kinetics of PS–DEG–AMTZ for Hg^{2+} (pH = 3, $[Hg^{2+}]$ = 0.005 mol/L).

Figure 3 Adsorption kinetics of PS–DEG–AMTZ for Ag^+ (pH = 3, $[Ag^+]$ = 0.005 mol/L).
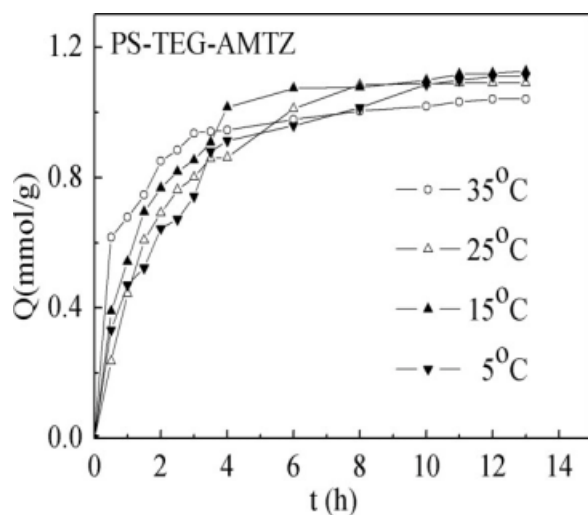
Figure 4 Adsorption kinetics of PS–TEG–AMTZ for Ag^+ (pH = 3, $[Ag^+]$ = 0.005 mol/L).

Synthesis of PS–DEG–AMTZ and PS–TEG–AMTZ

PS–DEG–AMTZ and PS–TEG–AMTZ were synthesized according to our previous work.[21] The structures of PS–DEG–AMTZ and PS–TEG–AMTZ are shown in Scheme 1.

ANAL. Found for PS–DEG–AMTZ: N, 2.14%; S, 10.37%. ANAL. Found for PS–TEG–AMTZ: N, 1.40%; S, 11.31%. FTIR (KBr, cm^{-1}) for PS–DEG–AMTZ: 3448 s, 3021 w, 2921 s, 2856 m, 1605 m, 1509 m, 1450 m, 1421 m, 1214 w, 1112 s, 830 m. FTIR (KBr, cm^{-1}) for PS–TEG–AMTZ: 3435 s, 3021 w, 2919 s, 2863 m, 1605 m, 1509 m, 1451 m, 1422 m, 1212 m, 1109 s, 827 m.

Adsorption kinetics

According our previous work,[22] PS–DEG–AMTZ and PS–TEG–AMTZ had higher adsorption capacities for Hg^{2+} and Ag^+ at pH 3, so we investigated the adsorption kinetics, isothermal adsorption, and selectivity adsorption for the two metal ions under this pH value in this experiment. Batch tests were performed to determine the adsorption kinetics. In the kinetic experiment, 30 mg of the resin was added to a mixture of 19 mL of a 0.1M acetate buffer solution (pH 3.0) and 1 mL of a 0.1M aqueous solution of metal ion. The mixture was shaken continuously in a thermostat-cum-shaking assembly at a defined temperature. At predetermined intervals, aliquots of 1 mL of solution were withdrawn, and the concentration of metal ions was determined by atomic absorption spectrophotometry. The adsorption capacities were calculated according to eq. (1):

$$Q = \frac{(C_0 - C)V}{W} \qquad (1)$$
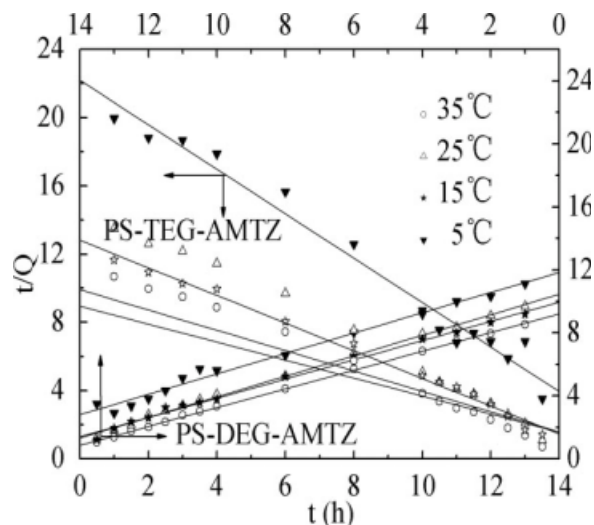
Figure 5 Pseudo-second-order kinetic model of PS–DEG–AMTZ and PS–TEG–AMTZ for Hg^{2+}.

where Q is the adsorption amount (mmol/g); C_0 and C are the initial concentration and the concentration of the metal ion in solution when the contact time is t (i.e., the equilibrium concentration), respectively (mmol/mL); V is the volume (mL); and W is the dry weight of resins (g).

Isothermal adsorption

The isothermal adsorption was also investigated by a batch experimental method. A typical procedure was as follows: a series of 50-mL test tubes were used. Each test tube was filled with 30 mg of the resin and 20 mL of a metal-ion solution of varying concentration and adjusted to the desired pH and temperature. After a shaking time of 24 h, the solution was separated from the adsorbent, and the concentrations of
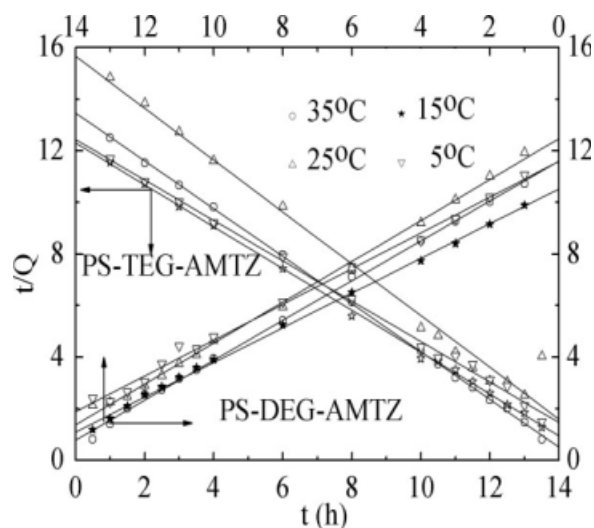
Figure 6 Pseudo-second-order kinetic model of PS–DEG–AMTZ and PS–TEG–AMTZ for Ag^+.

TABLE I
Parameters of the Pseudo-Second-Order Kinetic Models of PS–DEG–AMTZ and PS–TEG–AMTZ for Hg^{2+}

Temperature (°C)	Pseudo-second-order model of PS–DEG–AMTZ for Hg^{2+}			Pseudo-second-order model of PS–TEG–AMTZ for Hg^{2+}		
	k_2 (g/mmol)	Q_0 (mmol/g)	R^2	k_2 (g/mmol)	Q_0 (mmol/g)	R^2
35	0.38	1.82	0.9992	1.08	1.15	0.9959
25	0.29	1.66	0.9969	1.03	0.91	0.9950
15	0.24	1.77	0.9948	0.49	1.03	0.9916
5	0.14	1.68	0.9871	0.47	0.71	0.9743

metal ions were determined by atomic absorption spectrophotometry. The adsorption capacities were also calculated according to eq. (1).

Adsorption selectivity

To determine the adsorption selectivities of PS–DEG–AMTZ and PS–TEG–AMTZ under competitive conditions, the resins were put into contact with a binary mixture system in which the concentration of each metal ion was equal. The total concentration of the two kinds of metal ions was 4×10^{-4} M. Thus, 50 mg of the resin was shaken with a solution of binary mixture for 24 h. Then, the resin was separated by filtration, and the concentration of the metal ions in the binary mixture was determined by atomic absorption spectrometry. The selectivity index was defined as the ratio of the adsorption capacities of the metal ions in the binary mixture.

Reuse of the resins of PS–DEG–AMTZ and PS–TEG–AMTZ

To test the reusability of the resins, adsorption–desorption cycles of PS–DEG–AMTZ and PS–TEG–AMTZ for Ag^{+} were repeated five times with the same resin. The solution of 3% thiourea in 0.5 mol/L HNO$_3$ were used as the desorption medium. The resins adsorbing Ag^{+} were placed in 20 mL of desorbents and stirred for 10 h at room temperature. The final concentrations of Ag^{+} were determined with atomic absorption spectrophotometry. The desorption ratio was calculated from the amount of Ag^{+} adsorbed by the resin and the final concentration of Ag^{+} in the desorption medium.

RESULTS AND DISCUSSION

Adsorption kinetics

The adsorption kinetics of PS–DEG–AMTZ and PS–TEG–AMTZ for Hg^{2+} and Ag^{+} were determined at different temperatures. The adsorption rate curves are shown in Figures 1–4. The experimental results showed a rapid initial adsorption rate followed by a slower one, and the adsorption equilibriums were all established within 12 h.

The data in Figures 1–4 were treated by the pseudo-first-order Lagergren equation and a pseudo-second-order rate equation given in eqs. (2) and (3), respectively:

$$\log(Q_0 - Q) = \log Q_0 - \frac{k_1}{2.303}t \qquad (2)$$

$$\frac{t}{Q} = \frac{1}{k_2 Q_0^2} + \frac{1}{Q_0}t \qquad (3)$$

where k_1 is the rate constant of pseudo-first-order adsorption (h^{-1}), k_2 is the rate constant of pseudo-second-order adsorption (g/mmol), and Q_0 and Q are the adsorption amounts at equilibrium and at time t, respectively (mmol/g).

Both models were used to fit the kinetic curves, and the results show that the pseudo-second-order model was more suitable because the values of the linear correlation coefficient (R^2) could be regarded as a measure of the goodness-of-fit of the experimental data on the kinetic model. The straight lines obtained from the pseudo-second-order rate equations are shown in Figures 5 and 6. The parameters calculated according to the model are

TABLE II
Parameters of the Pseudo-Second-Order Kinetic Models of PS–DEG–AMTZ and PS–TEG–AMTZ for Ag^{+}

Temperature (°C)	Pseudo-second-order model of PS–DEG–AMTZ for Ag^{+}			Pseudo-second-order model of PS–TEG–AMTZ for Ag^{+}		
	k_2 (g/mmol)	Q_0 (mmol/g)	R^2	k_2 (g/mmol)	Q_0 (mmol/g)	R^2
35	0.77	1.29	0.9983	1.69	1.08	0.9997
25	0.46	1.26	0.9974	1.59	0.63	0.9808
15	0.41	1.48	0.9984	0.49	0.94	0.9990
5	0.26	1.44	0.9847	0.47	1.46	0.9969

TABLE III
ln k Versus $1/T$ Linear Equations and R^2 and E_a Values

	Linear equation	R^2	E_a (kJ/mol)
PS–DEG–AMTZ for Hg^{2+}	$E_a = -2743.8/T + 7.9738$	0.9591	22.81
PS–TEG–AMTZ for Hg^{2+}	$E_a = -2512.7/T + 8.1721$	0.9041	20.89
PS–DEG–AMTZ for Ag^{2+}	$E_a = -2885.3/T + 9.0376$	0.9497	23.99
PS–TEG–AMTZ for Ag^{2+}	$E_a = -3887.9/T + 13.29$	0.9307	32.32

tabulated in Tables I and II. From Tables I and II, we see:

1. For the same kind of resin, the values of k_2 of the resin for Hg^{2+} and Ag$^+$ increased with increasing temperature. These experimental phenomena could be attributed to the higher diffusion rate of metal ions at higher temperatures, so metal ions could approach and complex with the functional group much faster.

2. k_2 of PS–TEG–AMTZ for Hg^{2+} was higher than that of PS–DEG–AMTZ. Similar experimental phenomena were also observed in the case of Ag$^+$. These results are in accordance with the conclusion obtained in our previous article.[22] The experimental results illustrated that the introduction of a spacer arm produced an increase in the hydrophilicity of the functional group, which allowed for better contact between the metal ions in the aqueous solution and the chelating groups in the polymer and also increased the adsorption kinetics.

3. For the same kind of resin, the saturation adsorption capacities did not increase with increasing temperature as we expected. A possible explanation for this is that the diffusion rate of metal ions was enhanced by the increasing temperature, so metal ions could approach and contact the resin much faster at higher temperatures. Consequently, the complexes formed quickly on the surface and outer layer of the resin at high temperatures, which prevented the metal ions from diffusing into the inside of the resin, so the values of the adsorption capacities at the highest temperature were not the largest.

4. According to the pseudo-second-order rate equations, we calculated the theoretical adsorption capacity (Q_0; see Tables I and II). In our previous work,[22] the adsorption capacity of a chelating resin containing 2-amino-5-methyl-thio-1,3,4-thiadizole and without a spacer arm were studied. The adsorption capacity of the chelating resin that contained a spacer arm was much higher than that of the chelating resin that did not contain a spacer arm. This indicated that the coordination between the spacer arm and metal ions played an important role in the adsorption process.

According to the Arrhenius equation (ln $k_2 = -E_a/RT + \ln A$, where k_2 is the constant of adsorption obtained from pseudo-second-order rate equations, A is the pre-exponential factor, R is the gas
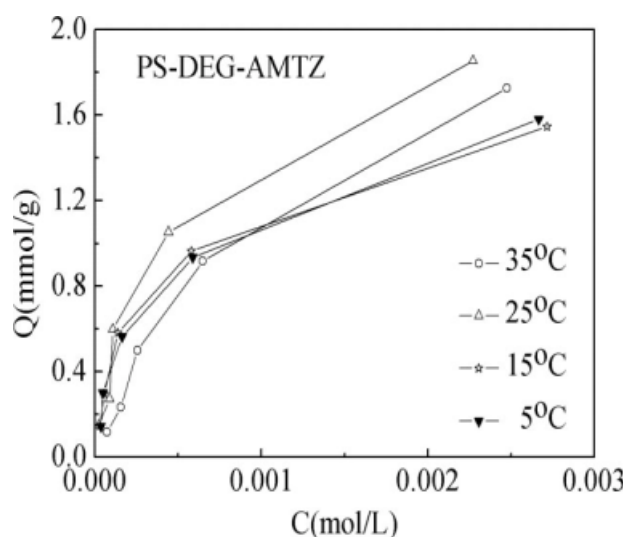

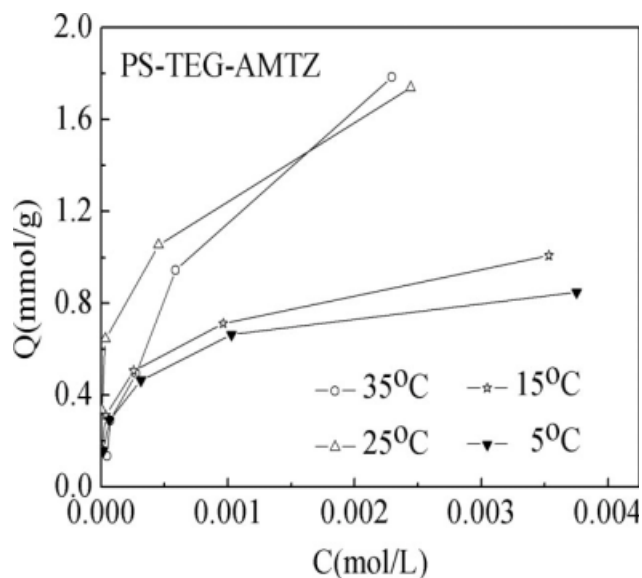**Figure 7** Adsorption isotherms of PS–DEG–AMTZ for Hg^{2+} (pH = 3).

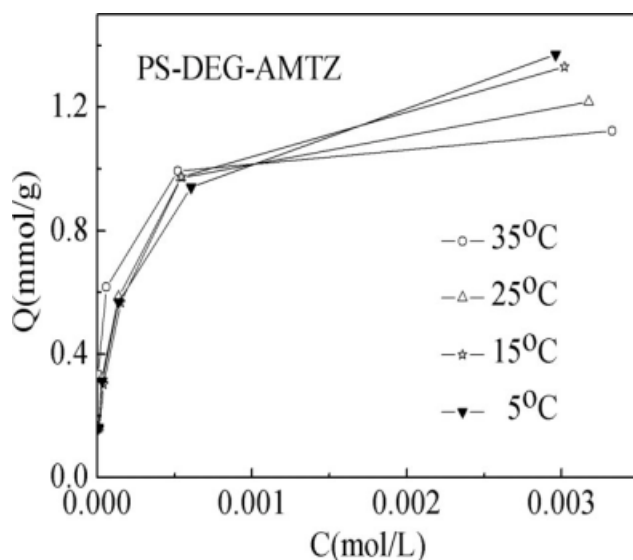**Figure 8** Adsorption isotherms of PS–TEG–AMTZ for Hg^{2+} (pH = 3).

Figure 9 Adsorption isotherms of PS–DEG–AMTZ for Ag$^+$ (pH = 3).

constant, T is the temperature, and E_a is the apparent activation energy of adsorption), by plotting ln k_2 against $1/T$, we could obtain straight lines. The linear equations and R^2 values are listed in Table III. All E_a values calculated from the linear slope were within 20.89–32.32 kJ/mol. These low activation energies, as compared to those of a typical chemical reaction of 65–250 kJ/mol, implied that the adsorptions of PS–DEG–AMTZ and PS–TEG–AMTZ for Hg^{2+} and Ag$^+$ were facile procedures.

Isothermal adsorption

The adsorption isotherms of PS–DEG–AMTZ and PS–TEG–AMTZ for Hg^{2+} and Ag$^+$ at four different temperatures were investigated (Figs. 7–10), and the data were analyzed with Langmuir [eq. (4)] and Freundlich [eq. (5)] equations, respectively.

$$\frac{C}{Q} = \frac{1}{bQ_0} + \frac{C}{Q_0} \tag{4}$$

$$\ln Q = \ln K_F + \frac{1}{n}\ln c \tag{5}$$

where Q is the adsorption capacity (mmol/g), Q_0 is the saturated adsorption capacity (mmol/g), C is the equilibrium concentration (mmol/mL), b is an empirical parameter, n is the Freundlich constant, and K_F is the binding-energy constant reflecting the affinity of the resin to metal ions.

All parameters in the Langmuir and Freundlich equations are tabulated in Tables IV–VII. As shown in Table IV, in the adsorption process of PS–DEG–AMTZ for Hg^{2+}, the value of R_L^2 (the linear correlation coefficient in Langmuir equation) was, in general, higher than that of R_F^2 (the linear correlation coefficient in Freundlich equation), which meant that the Langmuir model fit the results much better than the Freundlich model. In the case of PS–TEG–AMTZ for Hg^{2+}, the values of R_L^2 and R_F^2 were all above 0.9601 (see Table V). This meant the adsorption processes of PS–TEG–AMTZ for Hg^{2+} could be described by the Langmuir and Freundlich equations. In the adsorption process of PS–DEG–AMTZ and PS–TEG–AMTZ for Ag$^+$, the corresponding coefficients in the Langmuir equations were higher than those in the Freundlich equations (see Tables VI and VII), so we concluded that the Langmuir model fit the results much better than the Freundlich model; this indicated that the processes of adsorption were homogeneous and monolayer sorptions. In other words, the sorption of each sorbate molecule onto the surface had an equal sorption activation energy.

Competitive adsorption

Chelating resins possessed excellent adsorption and selectivity properties compared with other adsorbents. Many authors[23–25] have reported the selectivity of chelating resin for metal ions in binary mixture systems. The adsorption selectivities of PS–DEG–AMTZ and PS–TEG–AMTZ for Hg^{2+} and Ag$^+$ in binary mixture systems were investigated at 25°C. The experimental results are listed in Tables VIII and IX. Hg^{2+} and Ag$^+$ were adsorbed and Ni^{2+}, Zn^{2+}, Fe^{3+}, and Cd^{2+} were not adsorbed completely by PS–DEG–AMTZ and PS–TEG–AMTZ in the corresponding binary mixture systems. As shown in Tables VIII and IX, in the systems of Hg^{2+}–Pb^{2+}, Ag$^+$–Pb$^+$, and Ag$^+$–Cu^{2+}, the metal ions of Hg^{2+} and Ag$^+$ were adsorbed with priority by the resins. In the system of Hg^{2+}-Ag$^+$, the selective coefficients
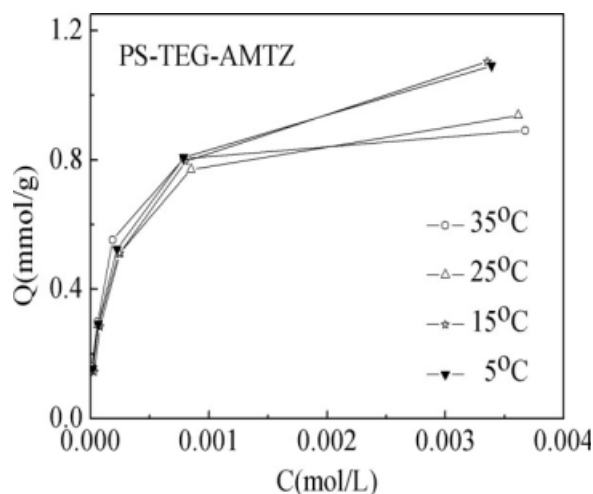

Figure 10 Adsorption isotherms of PS–TEG–AMTZ for Ag$^+$ (pH = 3).

TABLE IV
Parameters of the Langmuir and Freundlich Equations of PS–DEG–AMTZ for Hg^{2+}

Temperature (°C)	Q_0 (mmol/g)	$b \times 10^{-3}$	R_L^2	n	K_F	R_F^2
35	2.82	0.6642	0.9487	1.30	212.50	0.9536
25	2.20	2.3153	0.9812	1.78	67.35	0.9211
15	1.72	3.0463	0.9957	2.01	35.49	0.9255
5	1.79	2.5937	0.9904	1.97	37.14	0.9189

TABLE V
Parameters of the Langmuir and Freundlich Equations of PS–TEG–AMTZ for Hg^{2+}

Temperature (°C)	Q_0 (mmol/g)	$b \times 10^{-3}$	R_L^2	n	K_F	R_F^2
35	2.37	1.2632	0.9601	1.60	86.08	0.9653
25	1.80	8.1426	0.9867	3.90	8.05	0.9866
15	1.04	5.2994	0.9872	3.68	4.74	0.9979
5	0.88	5.1436	0.9949	3.27	5.17	0.9822

TABLE VI
Parameters of the Langmuir and Freundlich Equations of PS–DEG–AMTZ for Ag^{+}

Temperature (°C)	Q_0 (mmol/g)	$b \times 10^{-3}$	R_L^2	n	K_F	R_F^2
35	1.14	22.3318	0.9997	5.16	3.80	0.9587
25	1.26	8.6091	0.9990	2.86	11.22	0.9469
15	1.40	5.5985	0.9981	2.51	16.34	0.9619
5	1.44	5.7303	0.9944	2.68	13.73	0.9774

TABLE VII
Parameters of the Langmuir and Freundlich Equations of PS–TEG–AMTZ for Ag^{+}

Temperature (°C)	Q_0 (mmol/g)	$b \times 10^{-3}$	R_L^2	n	K_F	R_F^2
35	0.92	9.7641	0.9997	3.22	6.34	0.9299
25	0.98	5.9709	0.9985	2.95	7.45	0.9630
15	1.19	3.3695	0.9975	2.33	15.18	0.9562
5	1.16	4.4142	0.9967	2.62	11.17	0.9700

TABLE VIII
Adsorption Selective Coefficients of PS–DEG–AMTZ and PS–TEG–AMTZ for Hg^{2+} in Binary Mixture Systems at 25°C

System	Metal ion	PS–DEG–AMTZ		PS–TEG–AMTZ	
		Adsorption capacity (mmol/g)	Selective coefficient	Adsorption capacity (mmol/g)	Selective coefficient
Hg^{2+}–Ag^{+}	Hg^{2+}	0.22	1.57	0.22	1.47
	Ag^{+}	0.14		0.15	
Hg^{2+}–Pb^{2+}	Hg^{2+}	0.18	18	0.22	22
	Pb^{2+}	0.01		0.01	
Hg^{2+}–Cu^{2+}	Hg^{2+}	0.18	∞	0.23	∞
	Cu^{2+}	0		0	
Hg^{2+}–Ni^{2+}	Hg^{2+}	0.02	∞	0.23	∞
	Ni^{2+}	0		0	
Hg^{2+}–Zn^{2+}	Hg^{2+}	0.02	∞	0.18	∞
	Zn^{2+}	0		0	
Hg^{2+}–Fe^{3+}	Hg^{2+}	0.16	∞	0.17	∞
	Fe^{3+}	0		0	
Hg^{2+}–Cd^{2+}	Hg^{2+}	0.15	∞	0.17	∞
	Cd^{2+}	0		0	

pH = 3; metal-ion concentration = 4×10^{-4} mol/L.

Adsorption Selective Coefficients of PS–DEG–AMTZ and PS–TEG–AMTZ for Ag$^+$ in Binary Mixture Systems at 25°C

System	Metal ion	PS–DEG–AMTZ		PS–TEG–AMTZ	
		Adsorption capacity (mmol/g)	Selective coefficient	Adsorption capacity (mmol/g)	Selective coefficient
Ag$^+$–Pb^{2+}	Ag$^+$	0.21	10.5	0.20	20
	Pb^{2+}	0.02		0.01	
Ag$^+$–Cu^{2+}	Ag$^+$	0.21	10.5	0.20	∞
	Cu^{2+}	0.02		0	
Ag$^+$–Ni^{2+}	Ag$^+$	0.20	∞	0.19	∞
	Ni^{2+}	0		0	
Ag$^+$–Zn^{2+}	Ag$^+$	0.21	∞	0.19	∞
	Zn^{2+}	0		0	
Ag$^+$–Fe^{3+}	Ag$^+$	0.22	∞	0.19	∞
	Fe^{3+}	0		0	
Ag$^+$–Cd^{2+}	Ag$^+$	0.21	∞	0.19	∞
	Cd^{2+}	0		0	

pH = 3; metal-ion concentration = 4×10^{-4} mol/L.

of PS–DEG–AMTZ and PS–TEG–AMTZ for Hg^{2+} and Ag$^+$ were 1.57 and 1.47, respectively. All of the aforementioned data implied that PS–DEG–AMTZ and PS–TEG–AMTZ had good adsorption selectivities for Hg^{2+} and Ag$^+$, and the resins could be probably used in the extraction and separation of Hg^{2+} and Ag$^+$ from multi-ionic systems.

Reuse of PS–DEG–AMTZ and PS–TEG–AMTZ

Solutions such as 0.5 mol/L HNO$_3$, 1% thiourea in 0.5 mol/L HNO$_3$, 3% thiourea in 0.5 mol/L HNO$_3$, and 3% thiourea were chosen to desorb the metal ions adsorbed on the resin. The experimental results show that rates of elution with the aforementioned solutions were 40.5, 95.7, 100, and 59.8%, respectively. Therefore, a solution of 3% thiourea in 0.5 mol/L HNO$_3$ was used as the eluant to regenerate the resins. The results of five adsorption–desorption cycles are shown in Table X. After five adsorption–desorption cycles, the adsorption

TABLE X
Desorption and Regeneration Data

Resin	Reuse time	Adsorption capacity of the resin for Ag$^+$ (mmol/g)
PS–DEG–AMTZ	1	1.38
	2	1.32
	3	1.29
	4	1.29
	5	1.25
PS–TEG–AMTZ	1	1.09
	2	1.05
	3	1.02
	4	1.06
	5	1.03

pH = 3; [Ag$^+$] = 0.005 mol/L.

capacity had a slightly reduction. The data suggested that PS–DEG–AMTZ and PS–TEG–AMTZ were suitable for repeat use for more than five adsorption–desorption cycles.

CONCLUSIONS

The adsorption kinetics and adsorption isotherms of PS–DEG–AMTZ and PS–TEG–AMTZ for Hg^{2+} and Ag$^+$ were studied. The results show that the adsorption kinetics of the two resins could be modeled following the pseudo-second-order rate equation. The Langmuir equation could be used to model the adsorption process of the two resins for Hg^{2+} and Ag$^+$. The adsorption activation energies of the two resins for Hg^{2+} and Ag$^+$ were within 20.89–32.32 kJ/mol. The adsorption capacities of PS–DEG–AMTZ and PS–TEG–AMTZ for Hg^{2+} and Ag$^+$ were determined in binary mixture systems. The results show that the resins had good adsorption selectivities for Hg^{2+} and Ag$^+$. The resins of PS–DEG–AMTZ and PS–TEG–AMTZ were regenerated at least five times without considerable changes in the adsorption capacity for Ag$^+$.

References

1. McClain, A.; Hsieh, Y. J Appl Polym Sci 2004, 92, 218.
2. Ertan, E.; Gulfen, M. J Appl Polym Sci 2009, 111, 2798.
3. Fan, J.; Wu, C. L.; Xu, H. Z.; Wang, J. J.; Peng, C. Y. Talanta 2008, 74, 1020.
4. Baba, Y.; Ohe, K.; Kawasaki, Y.; Kolev, S. D. React Funct Polym 2006, 66, 1158.
5. Aydin, A.; Imamoglu, M.; Gulfen, M. J Appl Polym Sci 2008, 107, 1201.
6. Syamal, A.; Singh, M. M.; Kumar, D. React Funct Polym 1999, 39, 27.
7. Mokhodoeva, O. B.; Myasoedova, G. V.; Kubrakova, I. V. J Anal Chem 2007, 62, 607.
8. Lemos, V. A.; da Silva, D. G.; de Carvalho, A. L.; Santana, D. D.; Novaes, G. D.; dos Passos, A. S. Microchem J 2006, 84, 14.

9. Pramanik, S.; Dhara, S.; Bhattacharyya, S. S.; Chattopadhyay, P. Anal Chim Acta 2006, 556, 430.
10. Xiong, C. H.; Yao, C. P.; Wu, X. G. Hydrometallurgy 2008, 90, 221.
11. Pramanik, S.; Dhara, P. K.; Chattopadhyay, P. Talanta 2004, 63, 485.
12. Qu, R. J.; Wang, C. H.; Sun, C. M.; Ji, C. N.; Cheng, G. X.; Wang, X. Q.; Xu, G. J Appl Polym Sci 2004, 92, 1646.
13. Drago, R. S.; Gaul, J. H. Inorg Chem 1979, 18, 2019.
14. Collman, J. P.; Reed, C. A. J Am Chem Soc 1973, 95, 2048.
15. Lezzi, A.; Cobianco, S.; Roggero, A. J Polym Sci Part A: Polym Chem 1994, 32, 1877.
16. Lezzi, A.; Cobianco, S. J Appl Polym Sci 1994, 54, 889.
17. Sanchez, J. M.; Hidalgo, M.; Valiente, M.; Salvado, V. J Polym Sci Part A: Polym Chem 2000, 38, 269.
18. Qu, R. J.; Sun, C. M.; Ji, C. N.; Wang, C. H.; Zhao, Z. G.; Yu, D. S. Polym Eng Sci 2005, 45, 1515.
19. Sanchez, J. M.; Hidalgo, M.; Salvado, V. React Funct Polym 2001, 46, 283.
20. Cobianco, S.; Lezzi, A.; Scotti, R. React Funct Polym 2000, 43, 7.
21. Ji, C. N.; Qu, R. J.; Sun, C. M.; Wang, C. H.; Xu, Q.; Sun, Y. Z.; Li, C. X.; Guo, S. H. J Appl Polym Sci 2007, 103, 3220.
22. Ji, C. N.; Qu, R. J.; Xu, Q.; Sun, C. M.; Wang, C. H.; Cheng, Y. C.; Song, Y. P. J Appl Polym Sci 2009, 111, 2148.
23. Atia, A. A.; Donia, A. M.; Elwakeel, K. Z. React Funct Polym 2005, 65, 267.
24. Dev, K.; Pathak, R.; Rao, G. N. Talanta 1999, 48, 579.
25. Pramanik, S.; Dey, S.; Chattopadhyay, P. Anal Chim Acta 2007, 584, 469.